doi: 10.56761/EFRE2024.S3-O-019201

Numerical simulation of multiwave Cherenkov generators with periodic and biperiodic sections in X-band

V.A. Chazov, V.I. Koshelev, A.A. Petkun*

Institute of High Current Electronics SB RAS, Tomsk, Russia
vadim.chazov.2017@mail.ru

Abstract. The problem of generating radiation in X-band (up to 9.5 GHz) upon injection of a thin tubular electron beam (pulse duration up to 60 ns) into a cylindrical oversized slow-wave structure with a diameter of 130 mm was studied using a computer hybrid 2.5D code. The electrodynamic structure of the multiwave Cherenkov generator contained a diffraction reflector and 10–12 diaphragms in sections of the slow-wave structure. The output sections of the generator are presented by two options: with identical periods of diaphragms and with biperiodic diaphragm periods. In the periodic structure at a beam current of 9–20 kA and a diode voltage of 400–480 kV, the radiation pulse power of the radial component was obtained from 50 MW to 3.7 GW, depending on the length of the smooth tube between the diffraction reflector and the input section. An increase in radiation power using a biperiodic output section and variation of diffraction reflector tube in periodic generator, has been demonstrated.
Keywords: multiwave Cherenkov generator, diffraction reflector, biperiodic slow-wave structure.

1. Introduction

In high-power vacuum electronics, especially in relativistic BWOs and TWTs, an increasing of the oversize parameter D/λ makes it possible to significantly increase the radiation powers. Dividing the slow-wave structure (SWS) into several sections makes it possible to increase the efficiency of radiation generation by 1.5–2 times. This approach is implemented, in particular, in a multiwave Cherenkov generator (MWCG) [1]. Previously conducted experiments with a two-section MWCG with a diffraction reflector showed that a suitable choice of the distance between the input section and the reflector, the radiation power can be increased by 1.5 times. In particular, experiment for MWCG with a periodic output section [2], at a current of 13 kA and a diode voltage of 400 kV, a forward radiation power of the order of 1 GW in the 3 cm wavelength range (about 800 MW of the radially polarized component) was obtained by varying the length of the reflector tube. In experiments with an MWCG containing a biperiodic output section [3], 1.4 GW of forward radiation power (1.1 GW of the radially polarized component) was obtained at a current of 10 kA and a diode voltage of 470 kV. The radiation efficiency in both cases did not exceed 32%.

The purpose of the study is to compare the results of numerical simulation of a two-section MWCG with a diffraction reflector at ratio $D/\lambda \approx 4$ in the X-band of radially polarized radiation with previously obtained experimental results [2, 3]. Determine the influence of a smooth tube between the input section and the diffraction reflector on the radiation power parameters, and explain the differences in power parameters in the MWCG with the output periodic and biperiodic sections.

2. Numerical simulation of MWCG with periodic sections and with output biperiodic section

2.1. SWS geometry parameters and Cold Electrodynamic Simulation

Numerical calculations were carried out in a 2.5-D electromagnetic PIC code, where the fields of longitudinal electromagnetic resonances were preliminarily calculated (without taking into account ohmic power losses [4, 5]). Preanalysis of resonant electric fields of TM_{0nm} modes in the X-band were performed based on the scattering matrix method on rectangular longitudinal inhomogeneity in the Z-direction [4]. For both types of studied electrodynamic systems, a circular waveguide radius of R_w = 65 mm was used. The range of resonant frequencies is 7.8–9.6 GHz. The first electrodynamic system contained a diffraction reflector, including 4 diaphragms and two sections of a periodic SWS with 5 diaphragms in each section. The distance between the diffraction reflector and the first section L_r was variable in the range from 6 mm to 28 mm. The length of the drift tube between sections of the SWS is constant and equal to L_{dr} = 11.2 mm. The rectangular diaphragms in the sections had a width of w_g = 6.4 mm and a height of h_g = 4.1 mm, with a diaphragm period of d_1 = 12.4 mm. In the diffraction reflector, the period was equal to d_r = 18 mm, the width and height of the diaphragms were respectively equal to w_r = 9.6 mm and h_r = 4.6 mm.

The second electrodynamic system differed from the first only in the output biperiodic section - with periods d_1 = 12.4 mm and d_2 = 13.0 mm and additional diaphragms in each section (Fig. 1). The input section of the MWCG and the diffraction reflector are similar to the first system under study, and L_r = 11.6 mm and L_{dr} = 12.6 mm. For example, Fig. 1 shows an electrodynamic system of the second type with an electron beam at time moment of a current pulse of 36 ns (U_d = 475 kV, I_b = 10 kA, B = 2.4 T, r_b = 57 mm).

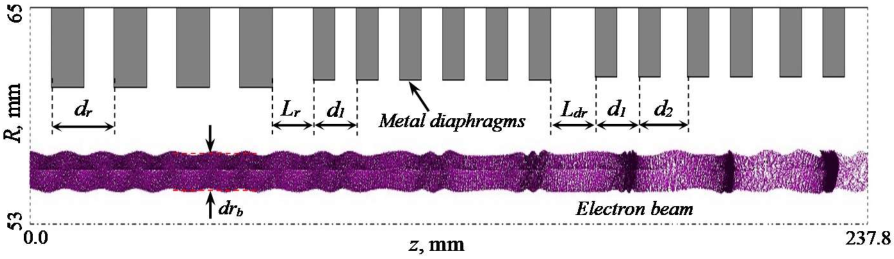

Fig. 1. Geometry of multiwave generator with output biperiodic section and a diffraction reflector in cylindrical coordinate system with an electron beam.

From 4 to 6 longitudinal TM resonances were taken into consideration, representing, in each case, the sum of the modes of the oversized waveguide at a given frequency. In the further description, each such resonance is associated with a classic name – TM_{0nm}. The mode numbers were counted from the frequency of π-type oscillations of TM_{01} mode (~ 9.58 GHz for the SWS with a period d_1) of an infinite periodic waveguide. On the dispersion curve (Fig. 2), the π-type oscillations of TM_{01} mode of the periodic structure d_1 correspond to an electron energy of $W_e \approx$ 240 keV (~ 400 kV of diode voltage for the geometry under study).

For the first type of MWCG, longitudinal resonances in the range from TM_{011} to TM_{013} and accompanying bulk resonances of the TM_{04m} modes were considered. In this case, regions of coupled modes could arise, where the fields simultaneously have a bulk and surface wave. The associated resonances in Fig. 3 are highlighted in the pale green region (~ 8.76 – 8.96 GHz). It should be noted that with an increase in the reflector tube, additional resonances of the TM_{01n} modes are possible, such as, for example, in the section indicated by the dashed line in Fig. 3, where two close resonances exists with noticeably different surface wave distributions – $TM_{011(a)}$ и $TM_{011(b)}$.

For a MWCG with a biperiodic output section, the phenomenon of coupled TM-resonances of surface and bulk waves is observed in the dispersion characteristics of infinite periodic and biperiodic waveguides (Fig. 4), where a narrow region of band gaps is formed. An example of the Q-factor spectrum calculated for the finite-length SWS with an output biperiodic section and a diffraction reflector (L_r = 11.2 mm и L_{dr} = 12.6 mm) is presented in Fig. 5. In addition to the Q-factor spectrum, the norms of the electromagnetic wave were determined, which together with the electrical components $E_r(r, z)$ and $E_z(r, z)$ described the TM-resonance in the approach under study.

2.2. PIC-Simulation of MWCGs with periodic and biperiodic output sections

Here we consider a direct comparison of experimental data [2, 3] with the results of a hybrid PIC-model, in which each TM resonance is characterized by frequency F_{res}, quality factor Q, electromagnetic wave norm N_e ($V^2 \cdot cm$) and electric field structure. The calculations estimated the power forward (P^+), backward (P^-) and total power ($P^- + P^+$) of radiation in the area limited by the space of the electrodynamic system. To analyze the process of interaction between the beam and the field, the amplitudes, the instantaneous frequencies of resonances f_i, the spectra S_i, and the frequency of the maximum of the emission spectrum f_0 were estimated. The parameters of the radiation power are given after generation reaches a stationary mode in the cross-section of a smooth tube beyond the output section.

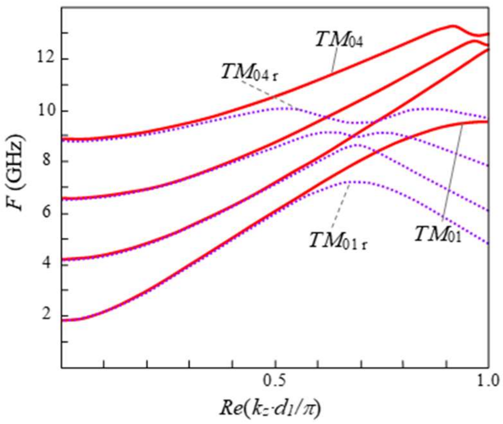

Fig. 2. Dispersion characteristics of TM modes of periodic structure d_1 (TM_{0n}) and diffraction reflector d_r (TM_{0m}).

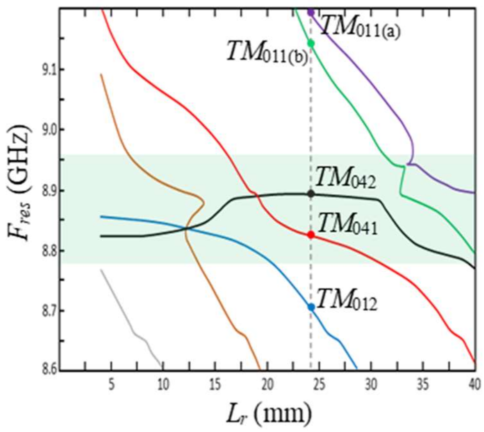

Fig. 3. Dependence of the frequency (F_{res}) of longitudinal TM resonances on the reflector tube length (L_r) in a sectionized periodic structure.

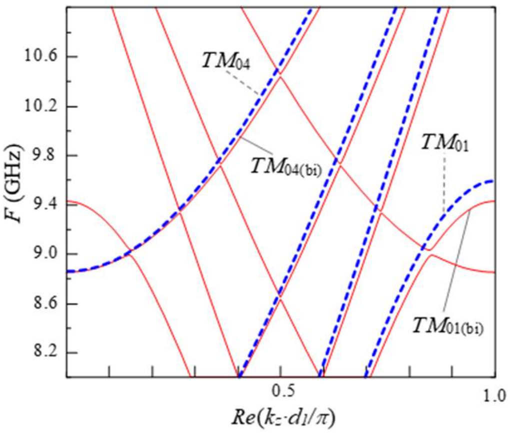

Fig. 4. Dispersion characteristics of TM modes of the periodic structure d_1 (dotted curves – TM_{0n}) and biperiodic structure $(d_1 + d_2)/2$ (solid curves – $TM_{0m(bi)}$).

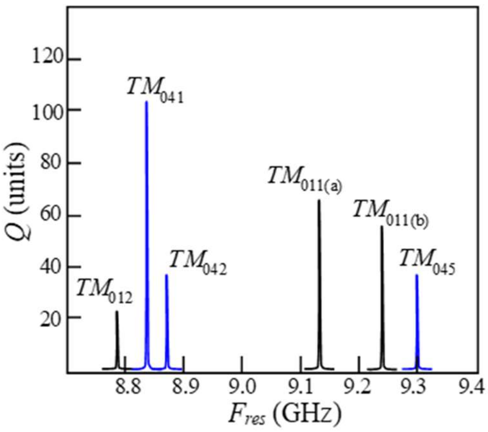

Fig. 5. Q-factor spectrum for TM-mode resonances of the MWCG with a diffraction reflector and output biperiodic section.

In the MWCG with a biperiodic output section, the following parameters of a tubular electron beam were studied: $W_e \approx 380$ keV, $I_b = 9.8–10$ kA, the middle beam radius and beam thickness varied – $r_b = 54–59.5$ mm and $dr_b = 0.5–3.5$ mm. The duration of the pulse leading front of the current was 5.5 ns and, accordingly, the voltage on the diode was $U_d = 475$ kV. Total pulse duration ~ 40 ns. The external magnetic field varied within the range of $B = 0.3–3$ T. For the calculated radiation power as a function of the external magnetic field (Fig. 6) and the beam radius (Fig. 7), there is some mismatch with the experimental data [3]. In particular, cyclotron absorption was observed in the experiment in the range of ~ 0.78–0.96 T (pale orange region in Fig. 6), and in the PIC model at ~ 0.98–1.1 T (pale green region in Fig. 6). In addition, in the range of 0.4–0.7 T before cyclotron absorption, the total radiation power in the experiment was almost 3 times lower, while at a magnetic field of more than 1 T, the experimental data and PIC modeling agree with a difference of 10–12%. The discrepancies in the results are apparently due to the failure to take into account asymmetric modes, which strongly influence the beam at low magnetic fields. The $P(r_b)$ dependence agrees well with experiment at $r_b \geq 56$ mm.

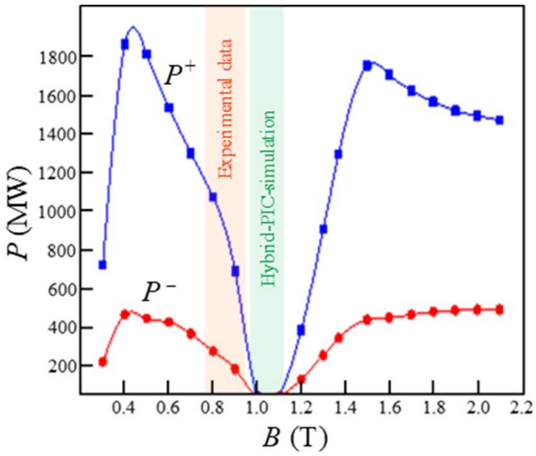

Fig. 6. Dependence of forward radiation power P^+ and backward power P^- on external magnetic field B for a beam with radius r_b = 56 mm and thickness dr_b = 1.5 mm.

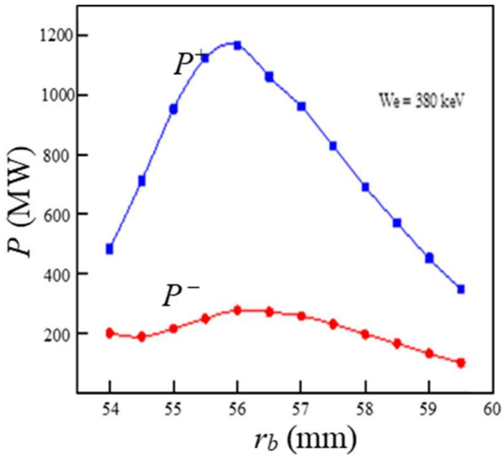

Fig. 7. Dependence of forward radiation power P^+ and backward power P^- on the beam radius with thickness dr_b = 1.5 mm in a magnetic field B = 1.37 T.

Stable generation of radiation reaching a stationary power value during the pulse at B > 1.0 T and $r_b \geq$ 56 mm occurred approximately 15 ns after the beam was injected. The radiation power as a function of a time is shown in Fig. 8 for a case close to the experiment: B = 1.37 T, I_b = 9.8 кA, r_b = 57 mm and dr_b = 2.5 mm. The shape of the obtained power signal is close to the experimental data [3], and the peak power value (1320 MW) in the PIC model exceeds the experimental value (1100 MW) by 20%. Fig. 9 shows the emission spectrum for the corresponding power signal together with the resonant frequencies of the TM_{0nm}. The maximum of the radiation spectrum $f_0 \approx$ 8.69 GHz practically coincides with the synchronization frequency of electromagnetic resonances f_s.

In the part of the study of the MWCG with a diffraction reflector and only periodic sections, the main attention was paid to the influence of the reflector tube on the parameters of the output radiation power. The following values were taken as reference points for comparison with experiments: L_r = 6, 8, 10, 11.2, 12, 13, 14.6, 17.6, 20, 24 and 28 mm. The frequency values depending on L_r data are presented in Figure 3. The quality factors of the TM resonances is in the range 10–120. Beam parameters: U_d = 400 kV ($W_e \approx$ 280 keV), B =1.5 T, I_b = 13 kA, dr_b = 1.5 mm, r_b = 58 mm.

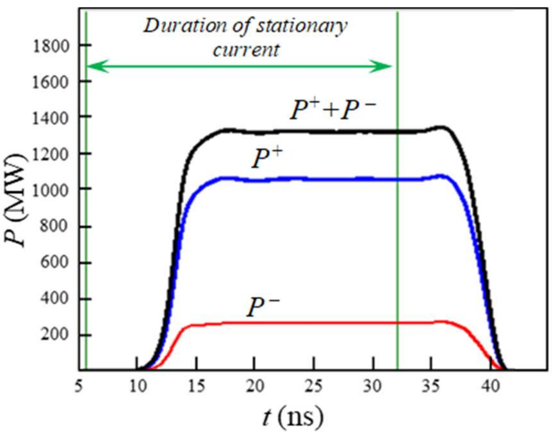

Fig. 8. Dependence of radiation power on time in a MWCG with a biperiodic output section at B = 1.37 T, I_b =9.8 kA, r_b = 57 mm и dr_b = 2.5 mm, U_d = 475 kV.

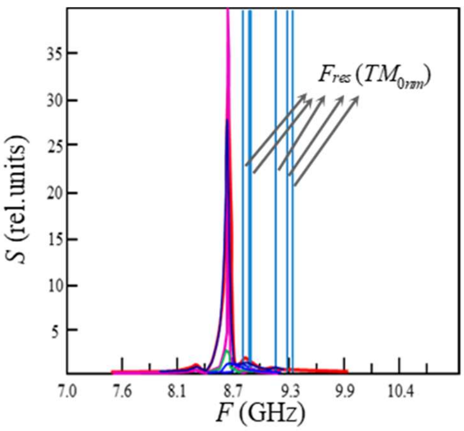

Fig. 9. Emission spectrum and resonant frequencies for MWCG with a biperiodic output section.

Fig. 10 shows the dependence of the radiation wavelength in the experiment and the wavelength of electromagnetic oscillations in the hybrid PIC model on the L_r value. The difference in wavelength values is no more than 6.5% (upward in the PIC model) for $L_r \leq 20$ mm. However, for the dependences of the forward radiation power on the length of the reflector tube (Fig. 11), significant differences were observed in the experiment and the PIC model: for values of $L_r \geq 14$ mm, the calculated power significantly exceeds the radiation power obtained in the experiment.

The wide discrepancy in results can be explained by the following factors:
Geometric differences of SWS in the experiment and in the PIC model. In the experiment, semitorus on rectangular pedestal rings were used as SWS elements, in contrast to the model, where rectangular pedestal rings were considered while maintaining the transverse cross-sectional area of the diaphragms. As the reflector tube increases, this factor greatly affects the spectrum of transverse modes of the structure. Only radially polarized field components were considered and asymmetric EH modes were not taken into account. In longitudinally inhomogeneous SWSs, the influence of simultaneous TM and EH modes on an electron beam can lead to noticeable competition during interaction with the beam and deformation of emitting bunches. In the experiment, the share of the cross-polarized radiation component was 20–30%.

The multiwave interaction mechanism was realized over the entire range of reflector tube lengths, and the average instantaneous radiation frequency shifted by 3–5% at $L_r \leq 13$ mm. The maximum value of the ratio of the average forward radiation power to the total radiation power – $\langle P^+/P \rangle$ was achieved in the range $L_r \approx 20$–24 mm and amounted to 93%.

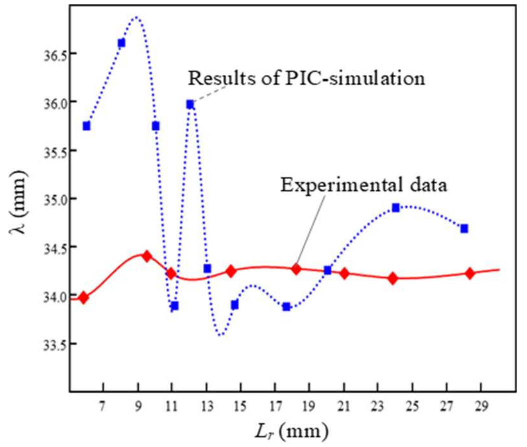

Fig. 10. Radiation wavelength in the experiment and in the PIC model depending on the reflector tube length in a periodic MWCG with a diffraction reflector.

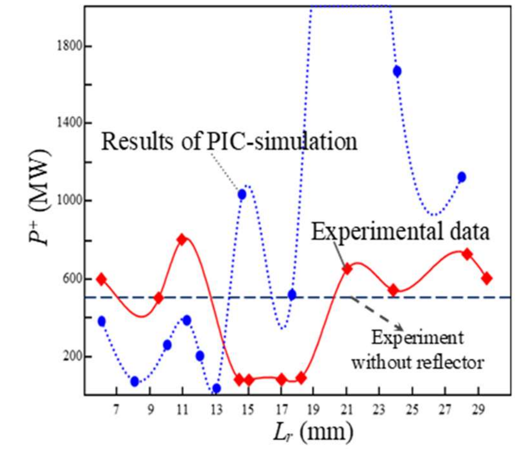

Fig. 11. Forward radiation power (radial component of polarization) depending on the reflector tube length in a periodic MWCG with a diffraction reflector.

3. Conclusion

Numerical studies of the MWCG with a diffraction reflector in the X-band based on a hybrid PIC code were carried out for two types of SWS: 1) periodic sections separated by a fixed drift tube and a with different distance between the first section and the reflector. 2) Periodic input section and biperiodic output section with fixed values of the drift and reflector tubes. In the 2nd type of MWCG, the results of simulating the radiation power (1320 MW) and experimental data (1100 MW) differ by 20%, and the average instantaneous radiation frequency in the model (8.693 GHz) differs from the experimental value in the spectrum (8.932 GHz) by 3%. A multiwave radiation mechanism is realized. In the 1st type of MWCG, a strong discrepancy between the results of the PIC model and the experiment was observed in terms of the forward power radiation (radial polarization) for values of the reflector tube $L_r >$ ~14 mm. This discrepancy is caused by a sum of factors associated both with the difference in the geometry under study in the model and experiments, and with the failure to take into account additional physical phenomena (asymmetric EH modes, power losses in output horn antenna). However, the qualitative behavior of the power function from the longitudinal inhomogeneity inside the structure (i.e., the reflector tube) with minima and maxima of the curve was observed similar to the experiment. A multiwave radiation mechanism was observed in the studied range of L_r.

Acknowledgement

This work was supported by the Ministry of Science and Higher Education of the Russian Federation (project no. FWRM-2021-0002).

4. References

[1] S.P. Bugaev, V.A. Cherepenin, V.I. Kanavets, A.I. Klimov, A.D. Kopenkin, V.I. Koshelev, V.A. Popov, and A.I. Slepkov, Relativistic multiwave Cerenkov generators, *IEEE Trans. Plasma Science*, vol. **18**, 525, 1990; doi: 10.1109/27.55924

[2] V.I. Koshelev, M.P. Deichuly, Reflectors influence on MWCG efficiency and radiation stability, *13th Int. Symposium on High-Current electronics*, Tomsk, Russia, 296–299, 2004

[3] M.P. Deichuly, V.I. Koshelev, V.M. Pikunov, V.A. Popov and A.A. Petkun, Multiwave Cerenkov generator with nonuniform slow-wave structures, *14th Int. Conf. on High-Power Particle Beams*, 287, 2002; doi: 10.1063/1.1530855

[4] M.P. Deichuly, V.I. Koshelev, A.A. Petkun, V.A. Chazov, Synchronization of electromagnetic resonances in terahertz Cherenkov generator, *Izvestiya vysshikh uchebnykh zavedenii. Fizika*, vol. **66**(6), 92, 2023; doi: 10.17223/00213411/66/6/11

[5] M.P. Deichuly, V.I. Koshelev, A.A. Petkun, and V.A. Chazov, Interaction of a relativistic electron beam and electromagnetic field in a terahertz Cherenkov generator with a Bragg reflector, *Journal of Communcation Technology and Electronics*, vol. **68**(12), 1430, 2023; doi: 10.1134/S1064226923120057